of the induction coil being tested is one-half the radius of Helmholtz coils [14].

11.1.1 Field Compensation Systems

Field compensation devices use coil systems to cancel variations of the external fields, mainly the Earth's natural field variations. Such systems work only when the field sources are distant. The requirements for the field gradient depend on the required quality of the field stabilization. One example may be a simple compensation system for computer monitors, which suppresses the field variations below 1 μT; it can work in a normal office environment with strong field sources located in ~20m distance. The field sensor may be an AMR magnetoresistor mounted directly on the monitor.

On the other hand, the system for thermal demagnetization of rock samples requires a magnetic vacuum below 0.5 nT; such a system should be located in a nonmagnetic building kilometers from the interference sources. The field sensors are nonmagnetic air-powered rotation magnetometers located inside the compensation system [10] or fluxgate sensors, which should be outside the coils [15].

Systems that are able not only to compensate the field changes or cancel the field completely but also to create independent artificial calibration field usually have the field sensors outside the coils. The sensor distance should be sufficiently large so that the field from the coil system is negligible; the external field gradients between the coil system and the sensors should be very small.

Active environmental noise-compensation systems for magnetically shielded rooms use induction coils, SQUIDs, or fluxgates as noise-reference sensors [4]. The shielding factor improvement of more than 40 dB in the frequency range of 0.1 to 10 Hz is achievable [16].

11.2 Magnetic Shielding

Magnetic shields are often an important part of high sensitivity magnetic measurements, testing, and calibration. This section reviews the theory and methods for efficient shielding static or slowly varying magnetic fields.

11.2.1 Magnetic Shielding Theory

Magnetic shielding provides a low-reluctance path guiding the magnetic flux around the region to be shielded (Figure 11.3). For the sake of simplicity,

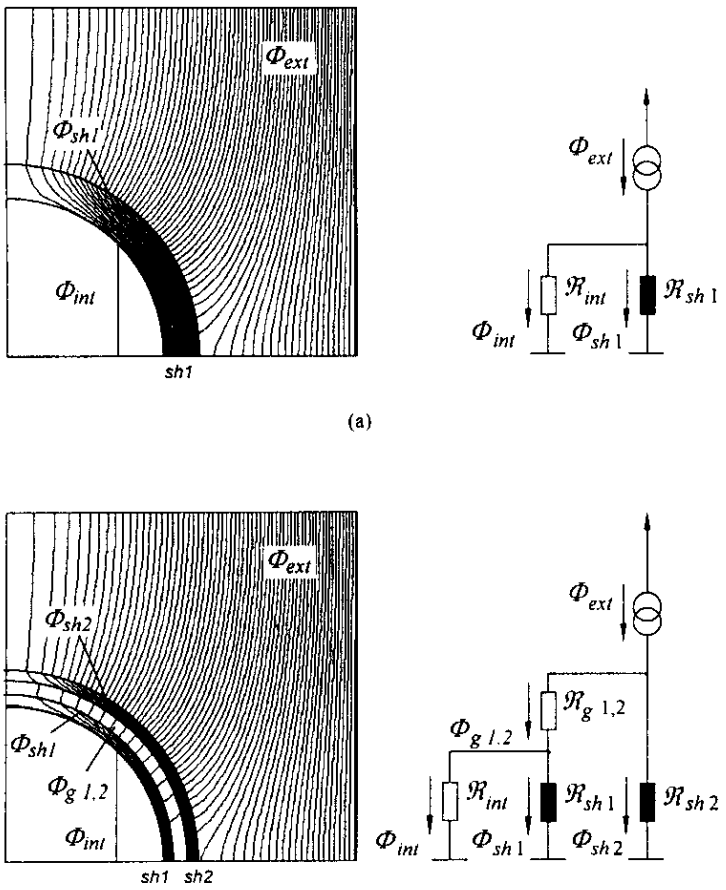

Figure 11.3 Transverse magnetic shielding: (a) single-shell and (b) double-shell cylindrical shields and their equivalent magnetic circuits. (Note that residual flux, Φ_{int}, is uniform.) The flux distributions are obtained numerically for $\mu = 100$.

it is generally assumed that a magnetic shield is placed in a uniform external field, and the permeability does not depend on the magnetic induction. Frequency, f, of the ambient field is assumed to be low enough to satisfy the quasi-static conditions: the skin depth $\delta \approx 1/\sqrt{\pi f \mu_0 \mu \sigma}$, is greater than the thickness t of a shield with the permeability μ and conductivity σ.

The shielding effectiveness is described by the two main parameters: the shielding factor, defined as the ratio of the external field to the residual

field (the field within the shielded region), and the uniformity of the residual field. It is obvious that the shielding effectiveness depends on the geometry, thickness, and permeability of the magnetic shell. Less obvious is that an introduction of air gaps between the shielding shells (see Figure 11.3) can greatly increase the shielding factor [17]. Mathematical solutions for the transverse magnetic field penetration into so-called ideal, single- and multiple-shell shields illustrate the preceding statements quantitatively.

11.2.2 Transverse Magnetic Shielding

Shielding assemblies such as a set of concentric spheres or infinitely long cylinders are considered ideal because they provide a uniformly reduced residual field (see Figure 11.3) [18].

For a single shell of thickness t, diameter D, and a constant relative permeability μ, the transverse shielding factor is given as follows [18]:

$$S_T \approx 1 + G\frac{\mu t}{D} \tag{11.6}$$

where $G = 4/3$ for a sphere and $G = 1$ for a cylinder. Exact mathematical solutions for the static magnetic field penetration into multiple-shell structures are cumbersome [19–21]. In the case of high permeability, $\mu >> 1$, and a relatively small thickness, $t/D << 1$, exact solutions can be reduced to simple forms. The transverse shielding factor for a double-shell shield becomes

$$S_{t\text{double}} \approx 1 + S_1 + S_2 + S_1 S_2\left(1 - \frac{W_1}{W_2}\right) \tag{11.7}$$

where $S_i \approx G\frac{\mu_i t_i}{D_i}$ is the transverse shielding factor for an individual shell, W_1 and W_2 are the volume of a sphere and cross-sectional area of a cylinder defined by the outer surface of layer 1 and inner surface of layer 2, respectively. The total shielding factor for the n-fold-shell shield is calculated in a similar way [21].

The transverse shielding factor for a finite-length cylindrical shield with open ends is reduced by the fringing fields penetrating through the openings [22]. Roughly, fringing fields are attenuated by a factor 10^3 per diameter distance from the open end [23].

Equation (11.7) represents the main principle of magnetic shielding with multiple shells [17]: Decoupling the shells ($W_1/W_2 << 1$) allows a multiplicative rather than an additive increase in shielding. As a result, the shielding factor for a set of thin concentric shells can be much greater than that for a single thick shell built with the same amount of material.

With thin multiple shells, the best minimum weight arrangement is when diameters of the shells grow in geometric progression, $D_j = \alpha D_i$, and the shielding material is distributed evenly among the shells [18, 19, 24]. Maximum shielding is obtained when the successive diameter ratio, α, is roughly 1.3 to 1.4 for spheres and 1.5 to 1.6 for cylinders [19]. A simple estimation of shielding with multiple-shell shields is suggested in [24]. A simple diagrammatic method of writing the shielding formulas is suggested in [25].

The transverse shielding factors and the residual field distribution for a set of elliptical cylinders are derived in [26]. If the external field is applied along the major axis of an elliptic cylinder with a 0.62–0.66 aspect ratio, then the shielding factor is increased, compared to a corresponding circular cylinder.

Cylinders with rectangular cross sections are treated in [27]. The transverse shielding factor for square cylinders can be calculated according to (11.6), where the diameter D equals the side of the square, $G \approx 0.70$ for a square cylinder in a perpendicular external field, and $G \approx 0.91$ for a square cylinder in a diagonal external field.

11.2.3 Axial Magnetic Shielding

11.2.3.1 Axial Shielding With Single-Shell Shields

In many cases, cylindrical shields cannot be positioned so that the axis of the shield is perpendicular to the ambient magnetic field (see Figures 11.4–11.6). Reference [22] suggests estimating the residual field within an axial (longitudinal) shield with the intrinsic field in a solid ellipsoid of revolution with the same aspect ratio and with an equivalent permeability averaged over the interior of the cylinder. Neglecting the effect of the openings, the axial shielding factor for an open cylinder is described in [22] as follows.

$$S_{a\text{open}} \approx 1 + N \cdot \mu_{\text{equiv}} = 1 + 4N \cdot \mu t/D \tag{11.8}$$

where N is the demagnetizing factor of a general ellipsoid [28], and $\mu_{\text{equiv}} = 4\mu t/D$ [Figure 11.4(a)]. Both circular and rectangular cylinders

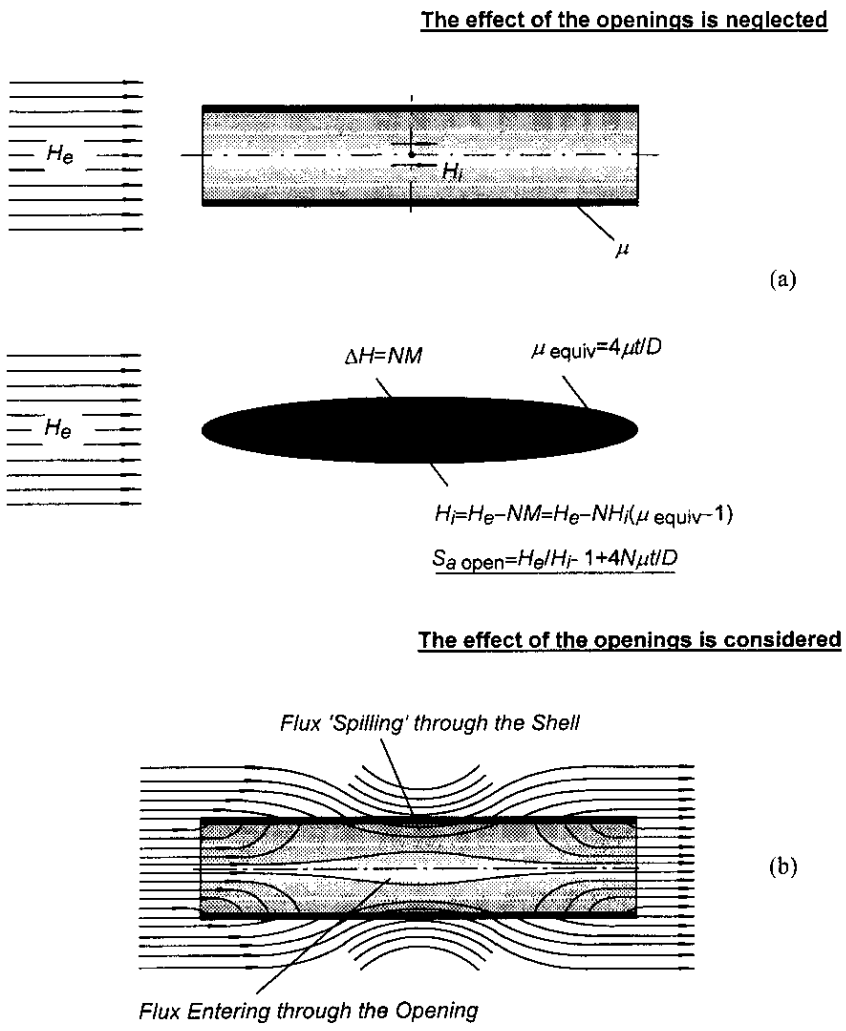

Figure 11.4 Axial shielding with open-ended cylinders. (a) Neglecting the field penetrating through the openings, the residual field can be approximated by the intrinsic field of an ellipsoid. (b) Simplified flux distribution around and within an open-ended cylinder.

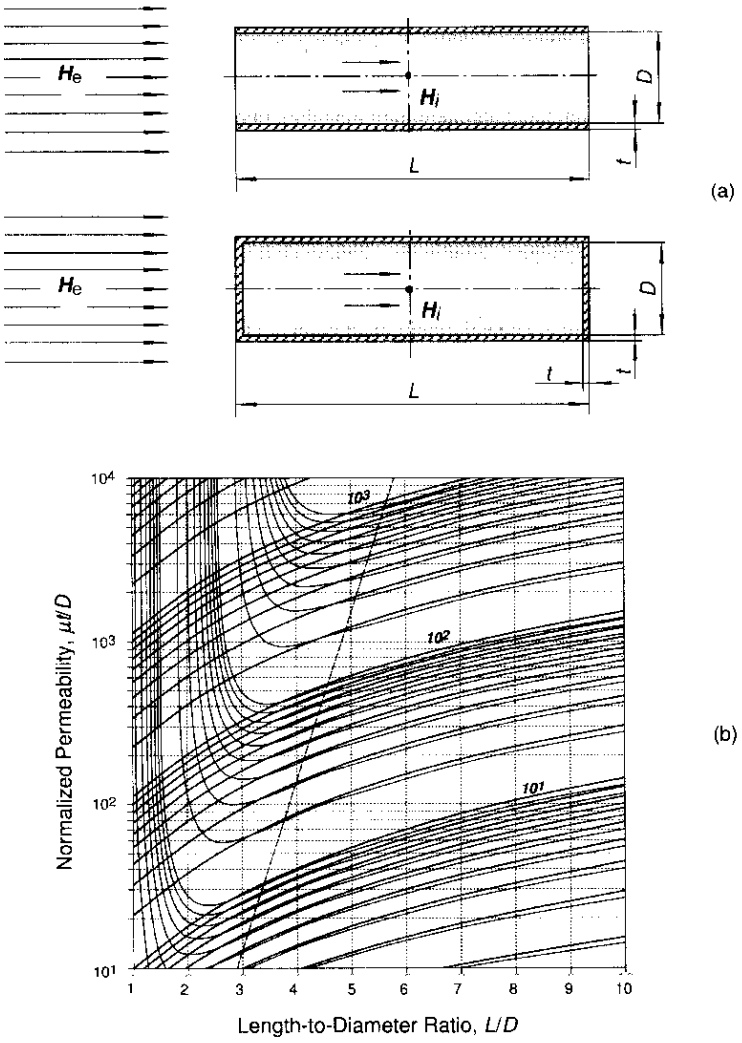

Figure 11.5 Axial shielding with single cylinders: (a) open-ended and closed cylinders; and (b) a numerically obtained chart (contour plot) describing the axial shielding factors (bold numbers) of open-ended cylinders (thin lines) and closed cylinders (thick lines).

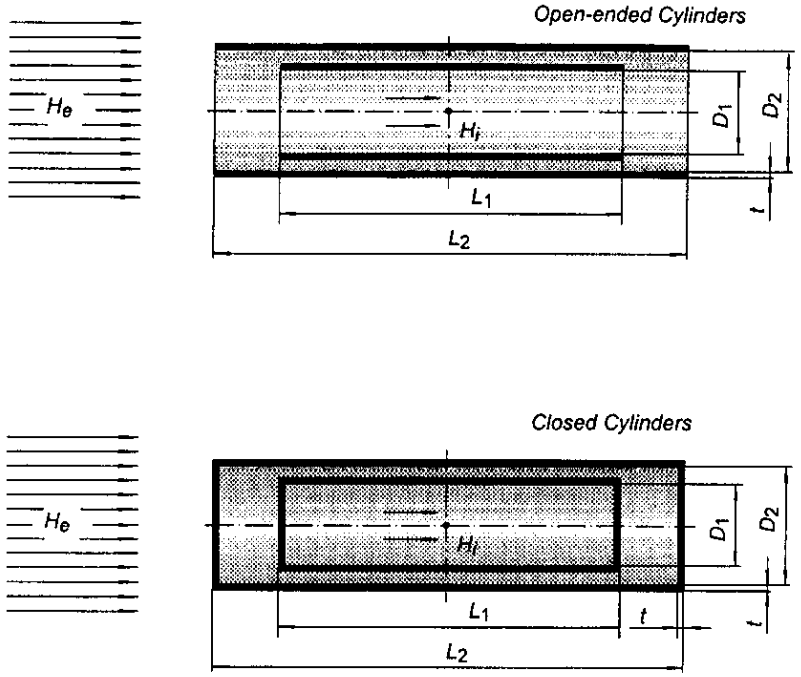

Figure 11.6 Double-shell cylinders: open-ended and closed cylindrical shields.

can be treated in a similar manner with the values of N for corresponding ellipsoids [22]; see also (2.22) through (2.24).

In the case of circular cylinders, it may be more accurate—and numerical calculations prove it [29]—to use demagnetizing factors calculated for rod [30] rather than for ellipsoid.

If the effect of the openings is still neglected, closed cylinders have a reduced axial shielding factor compared to (11.8) because their caps attract excess magnetic flux [22]:

$$S_{a\text{closed}} \approx \frac{1 + 4N \cdot \mu t/D}{1 + 0.5/(L/D)} \tag{11.9}$$

Numerical calculations [31] suggest a different formula, giving 15% to 20% lower shielding factors:

$$S'_{a\text{closed}} \approx \frac{1 + 4N_{\text{rod}} \cdot \mu t/D}{1 + (L/D)/100} \tag{11.10}$$

Let us now consider the effect of the openings. The openings dramatically reduce the axial shielding with relatively short open-ended cylinders. Fringing fields penetrating through the open ends [see Figure 11.4(b)] decay approximately exponentially and are attenuated by a factor of about 10^2 per diameter distance from the open end [22, 23].

The axial shielding factors for both open and closed cylinders ($D/t = 100$) versus the length-to-diameter ratio, L/D, and normalized permeability, $\mu t/D$, are shown in Figure 11.5 as a chart (contour plot) that is obtained numerically by a standard ANSYS® software package employing a finite element method. The chart illustrates behavior of the shielding factor as being affected by the shields' geometry and permeability. The two following geometry-related effects cause a decrease in the axial shielding factor: the effect of the openings for open-ended shields and decreasing the axial shielding factor by increasing the length for both open-ended and closed shields.

Although open cylinders generally are considered to provide a less uniform residual field, numerical calculations show that this situation is abruptly changed when the shields' aspect ratios approach the values depicted by the dashed line in the chart in Figure 11.5(b). In the region near the dashed line, the residual field becomes nearly uniform over a relatively wide shielded area and even outperforms the uniformity within corresponding closed cylinders.

11.2.3.2 Axial Shielding With Double-Shell Shields

Unfortunately, existing quasi-analytical estimations of axial shielding with multishell shields [21, 22, 25] predict results that are not in close agreement [21, 31]. On the other hand, employing special charts [32] describing shielding performance for the most widely applicable, canonical shielding structures can be a relatively accurate and time-saving alternative for many scientists and shield designers.

The charts shown in Figure 11.7 cover the case of double-shell open-ended cylinders (see Figure 11.6) with the aspect ratio of the outer cylinder, $L_2/D_2 = 5$; the ratio of diameters, $D_1/D_2 = 0.6$, and 0.9; the ratio of lengths, L_1/L_2, from 0 to 1; the normalized permeability, $\mu t/D_2$, from 10^1 to 10^4; and a constant thickness, $t = D_2/100$.

Figure 11.8 shows the case of closed cylindrical shields. There is no effect of the openings in this case, and the behavior of the axial shielding factor is much simpler. Shorter shields are considered in this case—compared to the case of open shields—because there normally is no need to make closed cylinders longer than four diameters.

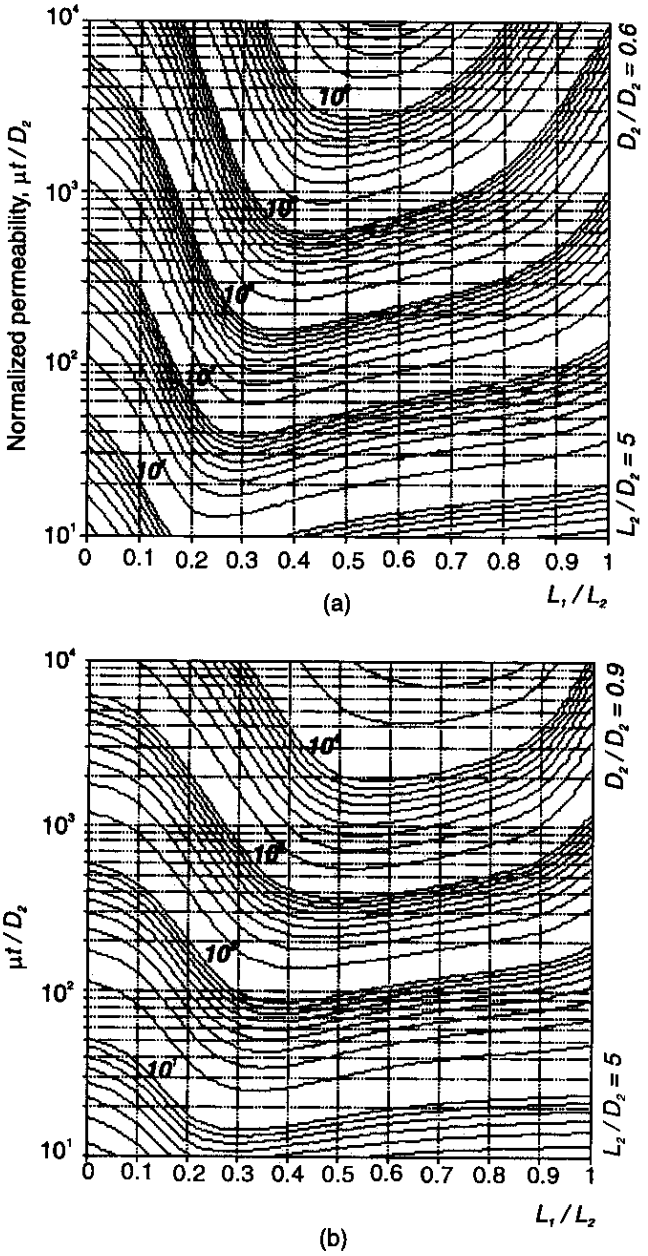

Figure 11.7 Charts for estimating the axial shielding factors for double-shell open-ended (see Figure 11.6) cylindrical shields.

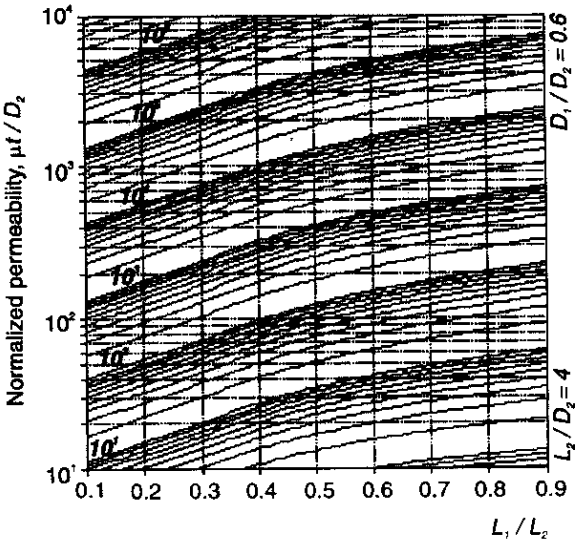

Figure 11.8 Charts for estimating the axial shielding factors for double-shell closed (see Figure 11.6) cylindrical shields.

Compared to the case of single cylinders (see Figure 11.5), two new geometry-related factors affect the axial shielding factor for double-shell open-ended shields: decoupling the shells by spaces between them and screening the ends of a shorter inner shell by a longer outer shell. Both factors increase the shielding factor.

It is important to note that shortening the inner shell is not always effective. For instance, it is worth choosing the same length for short shields with $L_2/D_2 \leq 3$, especially for high-permeability materials. In such a case, it is more important to reduce the effect of the openings by increasing the L_1/D_1 ratio of the inner shell rather than to screen the ends of the shell [32].

As in the case of single-shell shields, a better uniformity of the residual field can be obtained within a properly constructed double-shell open-ended shield [33].

11.2.4 Flux Distribution

Although a linear case is usually assumed in calculations, it is important to remember that the permeability depends strongly on the magnetic induction. Assuming that $\mu >> 1$, the maximum flux density within the shielding

material can be estimated according to [21], and corresponding permeability can be obtained from the normal magnetization curve given by manufacturers. Particular attention should be given to make the shielding shells—especially the outermost one—thick enough to avoid the dramatic decrease in the permeability when the material is saturated.

Considering $\mu >> 1$, the maximum flux density, $B_{m\text{transv}}$, within the material for a single-shell transverse cylindrical shield can be estimated as D/t times greater than the ambient field, B_0 [21]. Figure 11.9 shows how the ratio $B_{m\text{axial}}/B_{m\text{transv}}$ depends on the L/D ratio ($B_{m\text{axial}}/B_{m\text{transv}}$ is the ratio of the maximum flux density within the material for an axial single-shell cylindrical shield, to the same parameter for the corresponding transverse shield).

11.2.5 Annealing

Generally, once fabrication has been completed, the shielding shell should be annealed [34]. Annealing relieves mechanical stresses induced during fabrication. As a result, the shielding material reaches its optimum permeability. A standard annealing cycle for crystalline Permalloy materials includes heating above 1100°C in dry hydrogen for several hours and then cooling slowly. After the annealing has been completed, the shield or its parts should

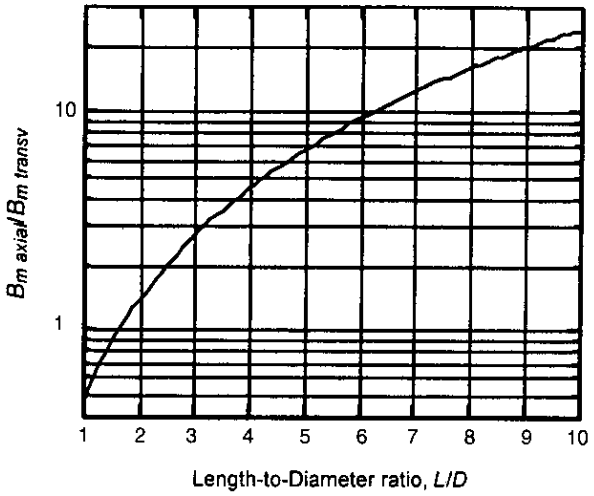

Figure 11.9 Dependence of the ratio of maximum flux density, $B_{m\text{axial}}$, within the material for axial single-shell cylindrical shields to the same parameter for corresponding transverse shields, $B_{m\text{transv}}$, on the length-to-diameter ratio, L/D.

be handled with care. Even a little mechanical stress can seriously reduce the permeability.

Modern, commercially available shielding materials, such as cobalt-based thin amorphous ribbons, are much less sensitive to mechanical stresses. Materials of this type make an excellent alternative to avoid the expensive annealing cycle in the manufacturing process. Care should be taken to avoid the saturation.

11.2.6 Demagnetizing

The lowest achievable dc field within a magnetic shield depends strictly on the magnetic history of the material after the annealing has been completed [23, 34]. The remnant magnetization of the shielding material can be reduced and the shielding factor against dc magnetic fields can be greatly increased by demagnetizing (degaussing) the shield *in situ.* Although demagnetization generally can be done magnetically or thermally, the magnetic method is usually easier. The magnetic state of the material is cycled by a field decaying slowly from the amplitudes that saturate the material to zero. Typically, the minimum dc residual field obtainable is 1 nT to 10 nT and is limited by stray fields from imperfections of the material's granular structure [21].

11.2.7 Enhancement of Magnetic Shielding by Magnetic Shaking

Magnetic shaking is an inexpensive and effective method to significantly increase the permeability and shielding performance against LF magnetic fields. Because of the application of a relatively strong, HF magnetic field, magnetic shaking keeps the domain walls within the material in continuous vibrant motion and allows the material to be more responsive to a slowly varying, weak ambient field. In other words, it is like sliding friction and static friction, the energy needed to move the domain walls is supplied by a fairly strong shaking field, therefore the permeability seen for the slowly varying low-level magnetic field becomes high [35, 36].

The most important key to effective magnetic shaking is the selection of the proper shielding material. Soft amorphous ferromagnets, such as Metglas® 2705M, with small magnetostriction and a highly rectangular hysteresis loop, seem to be the best choice. With Metglas® 2705M, shaking increases the effective incremental permeability 200- to 300-fold, resulting in μ from $4 \cdot 10^5$ to $6 \cdot 10^5$ [35]. Magnetic shaking is not effective if applied to Permalloy, in which incremental permeability is enhanced only several times [37].

Shaking efficiency strongly depends on the orientation of the magnetic anisotropy of the shielding material, namely, the anisotropy axis should be aligned along the corresponding shielding direction to achieve significant shielding enhancement [38]. The direction of the shaking field is less important. Shaking enhancement is observed with fields that are both parallel and perpendicular to the anisotropy direction. In the latter case, however, the shaking amplitude should be about 10 times greater, ~30 A/m versus ~3 A/m, to obtain maximum shaking enhancement [38].

References

[1] Jankowski, J., and C. Sucksdorff, *Guide for Magnetic Measurements and Observatory Practice*, Warsaw, Poland: IAGA, 1996.

[2] Brown, R. E., "Device for Producing Very Low Magnetic Fields," *Rev Sci. Instr.*, Vol. 39, 1968, pp. 547–550.

[3] Hechtfischer, D., "Homogenisation of Magnetic Fields by Diamagnetic Shields," *J. Phys. E: Sci. Instr.*, Vol. 20, 1987, pp. 143–146.

[4] Malmivuo, J., et al., "Improvement of the Properties of an Eddy Current Magnetic Shield With Active Compensation," *J. Phys. E: Sci. Instr.*, Vol. 20, 1987, pp. 151–164.

[5] Farrell, W., et al., "A Method of Calibrating Magnetometers on a Spinning Spacecraft," *IEEE Trans. Magn.*, Vol. 31, 1995, pp. 966–972.

[6] Kraus, J. D., *Electromagnetics*, 2nd ed., New York: McGraw-Hill, 1984.

[7] Firester, A. A., "Design of Square Helmholtz Coil System," *Rev. Sci. Instrum.*, Vol. 37, 1966, pp. 1264–1265.

[8] Alldred, J. C., and I. Scollar, "Square Cross Section Coils for the Production of Uniform Magnetic Fields," *J. Sci. Instrum.*, Vol. 44, 1967, pp. 755–760.

[9] Pajunpaa, K., V. Korepanov, and E. Klimovich, "Calibration System for Vector DC Magnetometers," *Proc. Imeko XIV World Congress*, Tampere, Finland, Vol. 4, 1998, pp. 97–102.

[10] Prihoda, K., et al., "MAVACS—A New System for Creating a Non-Magnetic Environment for Paleomagnetic Studies," *Geologia Iberica*, Vol. 12, 1988–1989, pp. 223–227.

[11] Everett, J. E., and J. E. Osemeikhian, "Spherical Coils for Uniform Magnetic Fields," *J. Sci. Instrum.*, Vol. 43, 1966, pp. 470–474.

[12] Spacecraft Magnetic Test Facility, NASA report X-754-83-9, Goddard Space Flight Center, Greenbelt, MD, Apr. 1984.

[13] Ripka, P., and A. Platil, "Analysis of Data From Three-Axis Magnetometer Calibrator," *Proc. SMC Conf.*, St. Petersburg, Russia, 1998, Vol. 2, pp. 60–66.

[14] Nissen, J., and L. E. Paulsson, "Influence of Field Inhomogeneity in Magnetic Calibration Coils," *IEEE Trans. Instrum. Meas.*, Vol. 45, 1996, pp. 304–306.

[15] McElhinny, M. W., et al., "A Large Volume Magnetic Field Free Space for Thermal Demagnetization and Other Experiments in Paleomagnetism," *Pure and Appl. Geophys.*, Vol. 90, 1971, pp. 126–130.

[16] ter Brake, H. J. M, R. Huonker, and H. Rogalla, "New Results in Active Noise Compensation for Magnetically Shielded Rooms," *Meas. Sci. Technol.*, Vol. 4, 1993, pp. 1370–1375.

[17] Rücker, A. W., "On the Magnetic Shielding of Concentric Spherical Shells," *Phil. Mag.*, Vol. 37, 1894, pp. 95–130.

[18] Thomas., A. K., "Magnetic Shielded Enclosure Design in the DC and VLF Region," *IEEE Trans. Electromagnetic Compatibility*, Vol. 10, 1968, pp. 142–152.

[19] Wills, A. P., "On the Magnetic Shielding Effect of Trilamellar Spherical and Cylindrical Shells," *Phys. Rev.*, Vol. 9, 1899, pp. 193–213.

[20] Wadey, W. G., "Magnetic Shielding With Multiple Cylindrical Shields," *Rev. Sci. Instrum.*, Vol. 27, 1956, pp. 910–916.

[21] Sumner, T. J., J. M. Pendlebury, and K. F. Smith, "Conventional Magnetic Shielding," *J. Phys. D: Appl. Phys.*, Vol. 20, 1987, pp. 1095–1101.

[22] Mager, A., "Magnetic Shields," *IEEE Trans. Magn.*, Vol. 6, 1970, pp. 67–75.

[23] Freake, S. M., and T. L. Thorp, "Shielding of Low Magnetic Fields With Multiple Cylindrical Shells," *Rev. Sci. Instrum.*, Vol. 42, 1971, pp. 1411–1413.

[24] Dubbers, D., "Simple Formula for Multiple Mu-Metal Shields," *Nucl. Instrum. Methods A*, Vol. 243, 1986, pp. 511–517.

[25] Gubser, D. U., S. A. Wolf, and J. E. Cox, "Shielding of Longitudinal Magnetic Fields With Thin, Closely Spaced, Concentric Cylinders of High Permeability Material," *Rev. Sci. Instrum.*, Vol. 50, 1979, pp. 751–756.

[26] Ohara, T., K. Koyama, and K. Imai, "Magnetic Shield Using Elliptic Cylindrical Shells," *Bulletin Electrotechnical Laboratory*, Vol. 45, 1981, pp. 20–34.

[27] Mager, A., "Magnetostatische Abschirmfactoren von Zylindern mit rechteckigen Querschnittsformen," *Physica*, Vol. 80B, 1975, pp. 451–463.

[28] Osborn, J. A., "Demagnetizing Factors of the General Ellipsoid," *Phys. Rev.*, Vol. 67, 1945, pp. 351–357.

[29] Paperno, E., and I. Sasada, "Optimum Axial Efficiency of Open Cylindrical Magnetic Shields," submitted for publication to *IEEE Trans. Magn.*

[30] Kobayashi, M., and Y. Ishikawa, "Surface Magnetic Charge Distributions and Demagnetizing Factors of Circular Cylinders," *IEEE Trans. Magn.*, Vol. 28, 1992, pp. 1810–1814.

[31] Paperno, E., H. Koide, and I. Sasada, "A New Estimation of the Axial Shielding Factors for Multi-Shell Cylindrical Shields," *J. Appl. Phys.*, Vol. 87, 2000, pp. 5959–5961.

[32] Paperno, E., "Charts for Estimating the Axial Shielding Factors of Open-Ended Cylindrical Shields," *IEEE Trans. Magn.*, Vol. 35, 1999, pp. 3940–3943.

[33] Paperno, E., I. Sasada, and H. Naka., "Self-Compensation of the Residual Field Gradient in Double-Shell Open Ended Cylindrical Axial Magnetic Shields," *IEEE Trans. Magn.*, Vol. 35, 1999, pp. 3943–3945.

[34] Bozorth, R. M., *Ferromagnetism*, New York: Van Nostrand, 1951.

[35] Sasada, I., S. Kubo, and K. Harada, "Effective Shielding for Low-Level Magnetic Fields," *J. Appl. Phys.*, Vol. 64, 1988, pp. 5696–5598.

[36] Sasada, I., et al., "Low-Frequency Characteristic of the Enhanced Incremental Permeability by Magnetic Shaking," *J. Appl. Phys.*, Vol. 67, 1990, pp. 5583–5585.

[37] Kelhä, V. O., R. Peltonen, and B. Rantala, "The Effect of Shaking on Magnetic Shields," *IEEE Trans. Magn.*, Vol. 16, 1980, pp. 575–578.

[38] Paperno, E., and I. Sasada, "The Effect of Magnetic Anisotropy on Magnetic Shaking," *J. Appl. Phys.*, Vol. 85, 1999, pp. 4645–4647.